CONDENSED MATTER PHYSICS

Observation of cavitation governing fracture in glasses

Lai-Quan Shen[1,2,3], Ji-Hao Yu[1,3], Xiao-Chang Tang[1,3], Bao-An Sun[1,2]*, Yan-Hui Liu[1,2,3], Hai-Yang Bai[1,2,3]*, Wei-Hua Wang[1,2,3]

Copyright © 2021 The Authors, some rights reserved; exclusive licensee American Association for the Advancement of Science. No claim to original U.S. Government Works. Distributed under a Creative Commons Attribution NonCommercial License 4.0 (CC BY-NC).

Crack propagation is the major vehicle for material failure, but the mechanisms by which cracks propagate remain longstanding riddles, especially for glassy materials with a long-range disordered atomic structure. Recently, cavitation was proposed as an underlying mechanism governing the fracture of glasses, but experimental determination of the cavitation behavior of fracture is still lacking. Here, we present unambiguous experimental evidence to firmly establish the cavitation mechanism in the fracture of glasses. We show that crack propagation in various glasses is dominated by the self-organized nucleation, growth, and coalescence of nanocavities, eventually resulting in the nanopatterns on the fracture surfaces. The revealed cavitation-induced nanostructured fracture morphologies thus confirm the presence of nanoscale ductility in the fracture of nominally brittle glasses, which has been debated for decades. Our observations would aid a fundamental understanding of the failure of disordered systems and have implications for designing tougher glasses with excellent ductility.

INTRODUCTION

Glassy materials are an essential ingredient for the modern world and find broad applications ranging from optics, architecture, electronics, to healthcare, etc. (*1*–*3*). However, inherent brittleness of glasses often leads to catastrophic failure, resulting in substantially lowered mechanical reliability of glassy parts (*4*–*6*). Therefore, understanding how glasses break is a topic of enormous fundamental and practical importance. Generally, breakage of materials is mainly triggered by the initiation and subsequent propagation of cracks, which is a process of numerous forefront scientific problems and encompasses a variety of fascinating physical phenomena (*7*–*12*). However, our knowledge of the fracture dynamics is far from complete. In particular, arising from the nature of structural disordering, unveiling the micromechanisms of fracture in glasses remains a challenging issue (*5*, *6*, *13*–*16*).

One of the fundamental questions in the glass research community is that whether glasses are capable of plastic flow during fracture (*6*, *15*–*20*). According to the framework of linear elastic fracture mechanics, the abrupt break of silicate glasses, an archetypal brittle material, is conventionally considered as perfectly brittle fracture (*4*). Nonetheless, some experiments and simulations suggested the existence of nanoscale ductility during crack propagation in silicate glasses (*17*, *18*), while some others claimed a completely brittle fracture behavior (*19*, *20*). These opposite standpoints thus lead to different theoretical understanding of fracture in glasses (*6*, *15*–*20*). To unlock the paradox, more convincing experimental evidence is urgently required.

Metallic glasses (MGs), an emerging class of glasses, provide a model system for the study of fracture in glassy materials owing to their simple atomic structures, compositional diversity, and wide range of fracture toughness values (*21*–*24*). Meanwhile, MGs show superior mechanical properties, such as high yield strength, large elastic limit, and extreme hardness (*25*, *26*), but limited ductility; in particular, tensile brittleness is the major hindrance for their engineering applications (*27*, *28*). Therefore, understanding how the catastrophic brittle fracture happens is one of the most resistant puzzles. Considerable efforts have been dedicated to the fractographic analysis to trace information on the fracture mechanisms (*15*, *29*–*35*). Various models, such as grease model, fluid meniscus instability, wavy crack, or crack-tip plasticity, have been proposed to describe the fracture process and formation mechanism of the diverse fracture surface patterns in MGs (*24*, *30*–*35*). However, there is still no well-established theory that is able to explain the intriguing fracture morphological features. Specifically, how the unique nanoscale periodic corrugation structures are formed in the "mirror" zones of the brittle fracture surfaces is a pressing problem (*24*, *32*–*37*). Recently, numerous calculations and simulations have recognized that cavitation is involved in the fracture of MGs and is believed to play an essential role in the failure of MGs, as well as other glassy materials (*3*, *36*–*47*). Nonetheless, direct evidence or experimental observation of cavitation in the fracture of glasses is hitherto lacking.

In this work, we report the experimental discovery of the cavitation mechanism that governs the fracture of glasses. On the basis of an ingenious sharp contact loading method, we study the fracture behavior of a wide range of glasses, including various MGs, polycarbonate (PC) glass, and silica glass (SiO_2), and demonstrate that glassy materials could share a common mechanism of fracture via cavitation. We present the clear-cut experimental observations of the fracture process from cavitation initiation to crack propagation and, ultimately, to fracture surface formation in MGs, and give a precise characterization on the cavitation-dominated crack propagation mode, including the nucleation, growth, and coalescence of nanocavities. Meanwhile, we clarify that it is the ordered coalescence of growing cavities that results in the periodic nanopatterned fracture surfaces featured by nanocorrugations in MGs. We further reveal that the cavitation-induced nanopatterns are also prevalent in nonmetallic PC and SiO_2 glasses and, hence, provide solid evidence for the presence of nanoscale ductility in the macroscopic brittle fracture of glasses. Our findings open up perspectives on how fracture proceeds in glasses and may pave an avenue toward the understanding of the many mysteries associated with the failure of disordered materials.

[1]Institute of Physics, Chinese Academy of Sciences, Beijing 100190, China. [2]Songshan Lake Materials Laboratory, Dongguan, Guangdong 523808, China. [3]College of Materials Science and Opto-Electronic Technology, University of Chinese Academy of Sciences, Beijing 100049, China.
*Corresponding author. Email: sunba@iphy.ac.cn (B.-A.S.); hybai@iphy.ac.cn (H.-Y.B.)

Downloaded from http://advances.sciencemag.org/ on March 31, 2021

RESULTS

Observation of cavitation-dominated crack propagation

To produce cracks in a controllable way, we upgraded the classical indentation fracture method (*4*, *48*). As illustrated in Fig. 1A, Vickers indentation was carried out on a sample attached to an inclined substrate. The inclination, together with the pyramid indenter, was introduced to induce opening-mode (mode I) loading that results in a cleavage emanating from the indent corner. Observation with a scanning electron microscope clearly shows that a V-shaped fracture surface and a straight crack along the opposite direction of the inclination were created (see Fig. 1B for the typical brittle $Fe_{78}Si_9B_{13}$ MG). Parallel nanoscale stripe patterns perpendicular to the crack propagation direction can be seen on both surfaces of the V-shaped fracture and form the periodic corrugation features (Fig. 1B and fig. S1, A and B), as observed on the brittle fracture surfaces obtained under tensile (fig. S2) and other loading conditions in many MGs (*24*, *32*–*35*). Meanwhile, the straight crack appears to be not a smooth line. To get a deeper insight, we used an atomic force microscope (AFM) with a sufficiently high resolution to examine the crack propagation process. Unexpectedly, we find that the crack is composed of a series of nanoscale cavities, and the width and depth of these cavities decrease gradually along the crack propagation direction, as shown in Fig. 1C. The zoom-in topographies reveal that these cavities gradually grow up from the crack front and coalesce in a regular head-to-tail mode, resulting in the wave-like crack edges (see Fig. 1D). Furthermore, around the crack front, each cavity is accompanied by a sharp

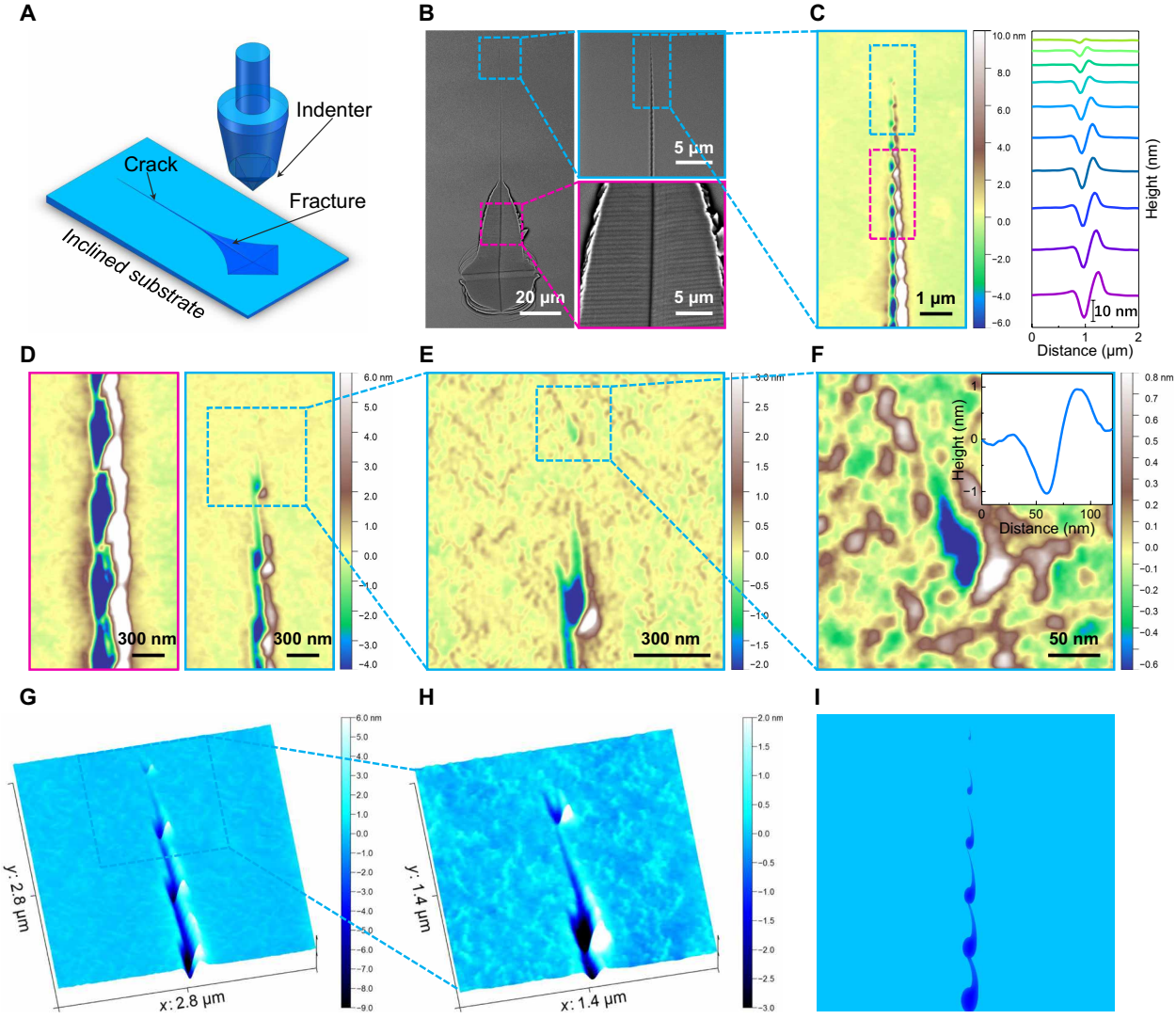

Fig. 1. Characterization of the cavitation governing fracture process in the Fe-based MG. (**A**) Schematic of the experimental setup. Indentation on an inclined substrate induces a cleavage opposite to the inclination direction. (**B**) Scanning electron microscope images after the inclined indentation in the Fe-based MG. The inclined indentation-induced cleavage (left) contains two parts: the straight crack (top right) and the V-shaped fracture surface (bottom right). Parallel nanoscale stripe patterns form on both surfaces of the V-shaped fracture. (**C**) Atomic force microscope (AFM) topographic image of the zoom-in straight crack (left). The straight crack consists of a series of nanoscale cavities. Height profiles of the top 10 cavities (right). (**D**) Zoom-in topographic images of the pink (left) and blue (right) rectangular zones in (C). (**E**) Topographic image of the crack tip. An isolated cavity nucleates ahead of the crack tip. (**F**) Topographic image of the cavity ahead of the crack tip. Inset: Height profile of the cavity. (**G** and **H**) Three-dimensional close-up topographies of another crack tip. Each cavity grows with an extending tadpole-like curved sharp tip and adjacent cavities coalesce along an organized path. (**I**) Schematic of the crack propagation. Crack propagation is in an ordered cavitation nucleation, growth, and coalescence mode.

Downloaded from http://advances.sciencemag.org/ on March 31, 2021

tip (see Fig. 1, D and E), indicating a "brittle" crack propagation. Amazingly, an isolated cavity with a width of 32 nm and a depth of 1.1 nm is found ahead of the sharp crack tip (Fig. 1, E and F), making it clear that plasticity exists ahead of the crack tip (*38*, *42*). The three-dimensional (3D) close-up topographies in Fig. 1 (G and H) provide further information about the cavitation behavior. As can be seen, discrete cavities nucleate ahead of the crack front, grow with curved sharp tips, and coalesce along an organized path; i.e., an extending tadpole-like curved tip grows from one edge of a cavity and links the other side of the growing cavity ahead of it (see also fig. S3), similar to the inference from simulation (*36*). It is intriguing to note that there exist nanoscale droplet-like pile-ups surrounding each cavity, corresponding to the white regions in Fig. 1 (D to H), indicating the occurrence of viscous flow or localized melting due to the dissipation of mechanical energy (*24*, *28*, *40*) during the cavitation process. On the basis of these observations, the dynamic crack propagation mode can be schematically demonstrated as the diagram shown in Fig. 1I. Cracking here seems to have a hierarchical structure (*12*, *14*), and the apparently linear macroscale crack proceeds in an organized nanoscale cavitation nucleation, growth, and coalescence mode (see also fig. S4). Unlike the expansion of spherical cavities or irregular cavitation process in simulation (*37*–*42*), here we find that cavitation precedes the onset of crack propagation and each nanocavity grows with a curved tadpole-like sharp tip and arranges one by one. Meanwhile, with the gradual growing and ordered coalescing of formed cavities, simultaneous multiple cavities nucleate equidistantly ahead of the crack tip.

To further characterize the cavitation-induced fracture process and unveil the formation mechanism of the fracture surface patterns, we studied the evolution of cracks with the increase of indentation strain. As shown in Fig. 2 (A to C), the crack opening width increases with increasing load, and, correspondingly, the separated small cavities linked by crack lines (Fig. 2A) evolve to successive cavities connection next to each other (Fig. 2, B and C). To gain a more precise identification, we carried out AFM tip scanning along the crack propagation direction and obtained topographic information inside the cracks. For the crack with a small opening width, the separated cavities are linked by curved grooves and extend inside the sample more deeply than the crack grooves (see Fig. 2D). With the increase of crack opening width, the cavities grow up and coalesce, resulting in the wave-like nanocorrugation structures along the crack (see Fig. 2, E and F), as observed on the fracture surfaces (Fig. 1B and fig. S1B). The above observations explain the longstanding puzzle of how the nanocorrugated fracture morphologies are formed in MGs and clarify that the periodic nanocorrugation patterns are not governed by the fluid meniscus instability or the wavy or oscillatory crack propagation but induced by the ordered cavitation process (*24*, *32*–*37*).

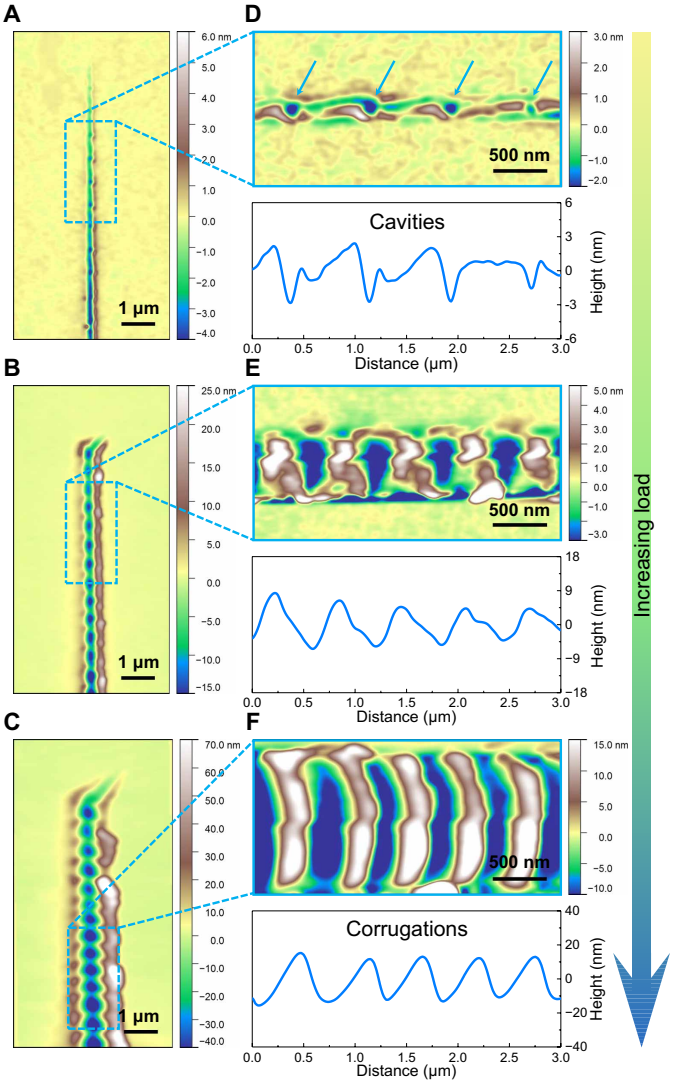

Fig. 2. Evolution of cracks with increasing load in the Fe-based MG. (**A** to **C**) Topographies of cracks at different inclined indentation strains. The crack opening widths increase with increasing load. (**D** to **F**) Topographies inside the cracks through AFM scanning along the crack propagation direction (top) and corresponding height profiles along the crack (bottom). The growth and coalescence of the cavities evolves to the wave-like nanocorrugation patterns. The arrows mark the cavities.

Cavitation behavior in different metallic glasses

To verify the generality of the cavitation behavior in different kinds of MGs, the same experiments were performed on the Mg-based, La-based, and Zr-based MGs with a variety of fracture toughness (*23*–*25*), respectively. Similar to that of the Fe-based MG, crack propagation in the brittle $Mg_{61}Cu_{28}Gd_{11}$ (K_{IC} ~ 2 MPa $m^{1/2}$, where K_{IC} is mode I fracture toughness) and $La_{55}Ni_{20}Al_{25}$ (K_{IC} ~ 5 MPa $m^{1/2}$) MGs is also governed by the cavitation mechanism, resulting in the periodic wave-like nanocorrugated morphologies (Fig. 3, A and B, and figs. S5 and S6). Moreover, as can be seen from Fig. 3C, the crack in the ductile $Zr_{64.13}Cu_{15.75}Ni_{10.12}Al_{10}$ (K_{IC} ~ 50 MPa $m^{1/2}$) MG is also composed of multiple nanocavities, but the shape of the cavities is not as regular as that observed in brittle MGs. In addition, the pile-ups surrounding the cavities are more obvious, indicating the more significant viscous flow during the cavitation process in the ductile Zr-based MG. In contrast to the sharp tips in the brittle MGs, the crack tip for the Zr-based MG is blunt and adjacent cavities are separated by blunt walls (Fig. 3C), indicating a "ductile" crack propagation. At higher load, the coalescence of adjacent cavities occurs through the necking or tearing of the viscous wall between them (Fig. 3D), resulting in the viscous fluid-like morphology. Nonetheless, cracking here is not a process dominated by the fluid meniscus instability (*24*, *30*), but a process undergoing the growth and coalescence of nanocavities. Therefore, we can infer that, similar to brittle MGs, the tensile fracture of ductile MGs also arises from the cavitation instability. The difference lies in that the growth and coalescence

Downloaded from http://advances.sciencemag.org/ on March 31, 2021

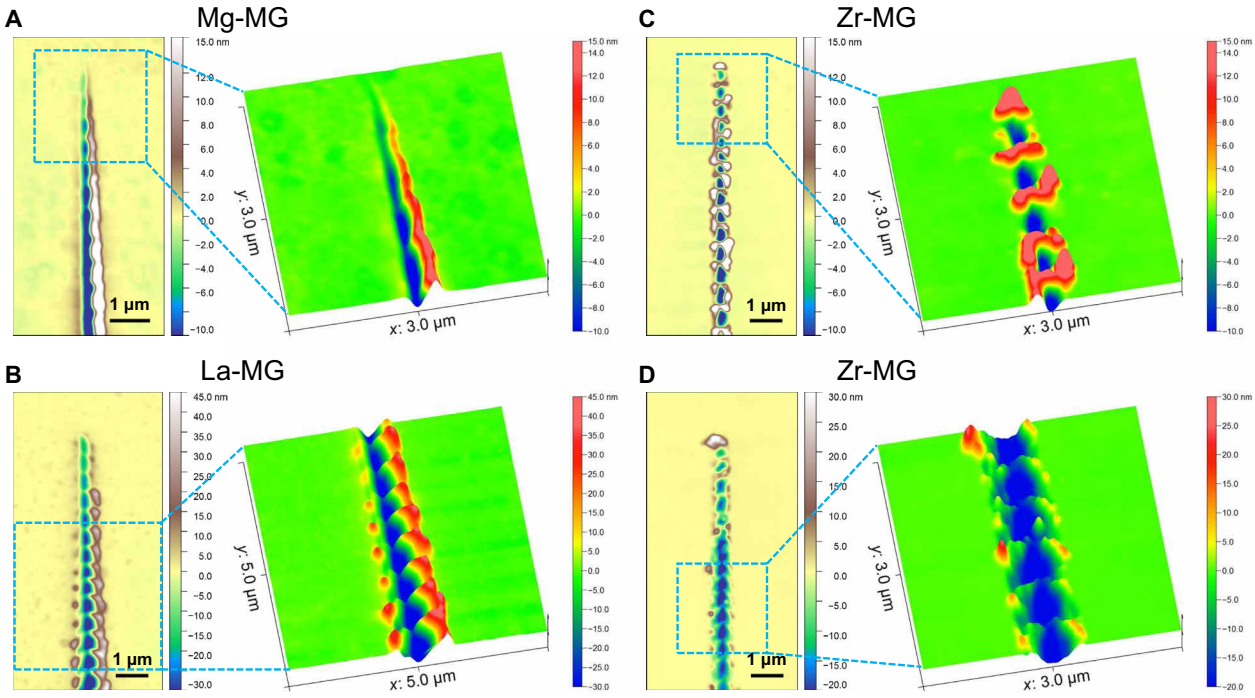

Fig. 3. Cavitation governing crack behavior in the Mg-based, La-based, and Zr-based MGs. (**A** and **B**) Topographies of the cracks in the Mg-based and La-based MGs, respectively. The cracks are composed of coalescent cavities, and the regular wave-like nanocorrugations form along the cracks. (**C**) Topographies of the crack in the Zr-based MG. The crack tip is blunt, and cavities forming the crack are separated by blunt walls. (**D**) Topographies of the crack at higher load in the Zr-based MG. Adjacent cavities coalesce through necking or tearing of the viscous wall between them.

process of cavities in ductile MGs are accompanied by the more significant viscous flow, which ultimately results in the diverse fracture morphologies (*24*).

So far, we demonstrate that cavitation is a prevalent mechanism in the fracture of a wide range of MGs. The cavitation phenomenon we revealed suggests that the catastrophic failure of MGs is not a simple shear-band runaway event (*28*, *40*), but a successive process involving the nucleation, growth, and coalescence of nanocavities. Furthermore, as can be seen from figs. S4 and S5, even though the crack is a microcrack or there exists a disturbance during crack propagation, the cracking process still follows the cavitation mechanism, indicating the robustness of the intrinsic cavitation capacity. Considering the fact that nearly all MGs exhibit apparently brittle failure in tension regardless of their toughness values (*24*, *27*, *28*), the common cavitation behavior of tensile fracture implies that the intrinsic cavitation mechanism is the key to understanding the tensile brittleness of MGs.

Cavitation-induced nanopatterns in nonmetallic glasses

Could this cavitation mechanism be generalized to the failure of conventional non-MGs? In the following, we focus on the fracture of PC and SiO_2 glasses. As shown in Fig. 4A, the inclined indentation could induce a wide V-shaped fracture surface in PC. In analogy to those in the MGs (figs. S1A and S6A), AFM imaging obviously shows the periodic nanocorrugations along the crack propagation direction, where the two opposing surfaces of the V-shaped fracture exhibit peak-to-peak and valley-to-valley matched fracture morphologies (Fig. 4B). Therefore, the cavitation-induced nanocorrugations are not unique to MGs. In addition, as shown in Fig. 4C and fig. S7, periodic nanoarray patterns are also observed. These kinds of patterned structures are similar to the common dimple structures on the fracture surfaces of MGs (*24*), but their formation mechanism is still missing. By continuous scanning over a sufficiently large area on the fracture surface, we captured the border of the nanoarray patterns and found that there is a transition from nanocorrugations to nanoarrays (see Fig. 4D). The findings show that these nanoarray patterns are compound structures resulting from the intersection of two nanocorrugation series along different orientations (see also fig. S7A), indicating that the nanoarray patterns on the fracture surfaces still originate from the cavitation mechanism.

To address the issue of whether ideal brittle silicate glasses exhibit ductility during fracture (*6*, *15*–*20*), we further carefully inspected the fracture behavior of SiO_2. As shown in Fig. 4E, a straight V-shaped crack groove is obtained after the inclined indentation. Unexpectedly, vanishingly weak cavity traces and periodic nanocorrugations can also be found on the fracture surfaces (Fig. 4E and fig. S8, A and B). AFM tip scanning along the crack clearly presents the out-of-plane nanocorrugations with a maximum amplitude of 3 nm (Fig. 4F). It should be noted that the amplitudes of nanocorrugations on the two opposing surfaces of the V-shaped fracture are unequal, similar to those in the MGs (figs. S4D and S6B), owing to the asymmetric coalescence mode of cavities, as described in Fig. 1. These findings explicitly show that the ductile damage process (cavitation process) also exists in the fracture of nominally ideal brittle covalent SiO_2 and thus confirm the occurrence of plastic flow instead of perfectly brittle fracture via sequential bond rupture (*4*, *6*, *15*). Compared to the previous conflicting conclusions (*6*, *15*–*20*), the regular and periodic cavitation-induced nanocorrugations provide the clear and convincing evidence for the presence of nanoscale ductility in the fracture of glasses, thus clarifying the long-lasting controversy (*6*, *15*–*20*).

Downloaded from http://advances.sciencemag.org/ on March 31, 2021

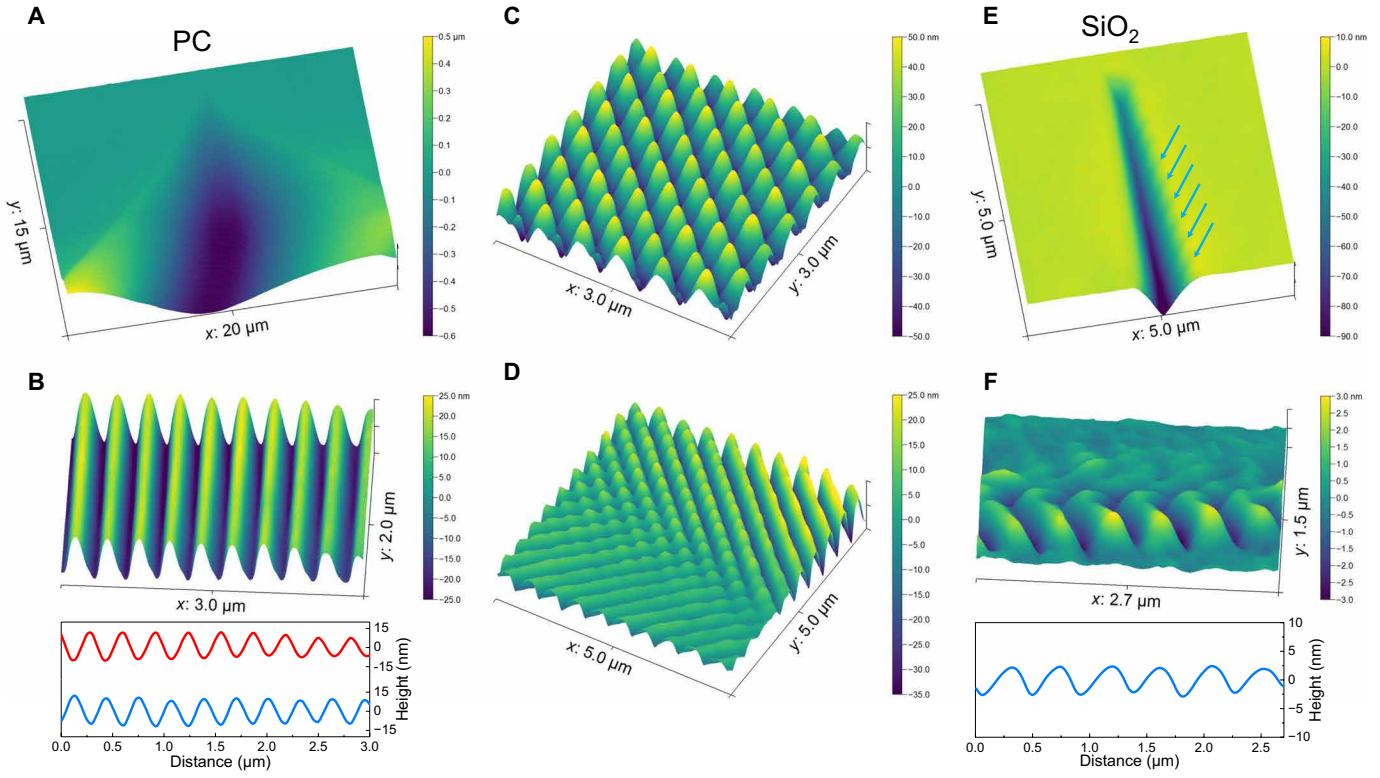

Fig. 4. Cavitation-induced nanostructured fracture surfaces in PC and SiO_2 glasses. (**A**) V-shaped fracture surface after the inclined indentation in PC. (**B**) Nanocorrugations on the fracture surface (top) and height profiles on the two opposing surfaces of the V-shaped fracture in PC (bottom). Periodic wave-like nanocorrugations form on both surfaces of the V-shaped fracture and result in the peak-to-peak and valley-to-valley matched fracture morphologies. (**C**) Periodic nanoarray patterns on the fracture surface of PC. (**D**) Nanostructure evolution on the fracture surface of PC. The nanoarray structure results from the intersection of two series of orthogonal nanocorrugations. (**E**) V-shaped crack groove after the inclined indentation in SiO_2. The arrows mark the cavity traces. (**F**) Nanocorrugations on the fracture surface (top) and corresponding height profile of SiO_2 (bottom).

DISCUSSION

The above results indicate that irrespective of the glass type, the dynamic (mode I) fracture of glasses can proceed through a generalized cavitation mechanism, challenging the traditional concepts of how glasses break. In contrast to the inconsistencies in simulations (*37*–*42*), our findings suggest that the universality of cavitation occurrence is not composition or chemical element dependent, but the chemical compositions do have an effect on the intrinsic plastic flow ability of glasses, thus affecting the detailed growth and coalescence process of cavities during fracture. Furthermore, we note that a commonality of brittle glasses is the nanocorrugated fracture morphologies and the amplitude of nanocorrugations induced by the cavitation process is positively correlated with the toughness for different types of brittle glasses (see Fig. 5), where the correlation can be fitted by exponential equation $y = A\exp\left(-\frac{x}{x_0}\right) + y_0$ (fitting parameters $A = -22.09$, $x_0 = 0.78$, $y_0 = 25.03$, and $R^2 = 0.99$). This means that the degree of plastic flow during the cavitation process depends on the intrinsic toughness of glasses, implying that the inherent fracture resistance is associated with the intrinsic plasticity (*22*, *41*), even for brittle glasses with rather limited damage tolerance. Moreover, the nanoscale ductility reflected by the cavitation behavior indicates that glasses are capable of ductile fracture, even though they show tensile brittleness on the macroscale. Therefore, we can anticipate that when the sample size is reduced to the nanoscale, in particular, comparable to that of cavitation, glasses will exhibit tensile plasticity, as observed recently (*49*, *50*).

It is worth emphasizing that the crack-induced wave-like corrugation patterns observed here differ fundamentally from those previous studies, including corrugations arising from oscillatory instabilities or crack front waves (*7*–*10*, *14*), even though they exhibit a remarkable morphological similarity. The wavy crack trajectories caused by the oscillatory instabilities of rapid cracks (*7*, *8*) and the undulating fracture surface patterns resulting from the interaction of the crack tips with front waves (*9*, *10*) are typical brittle fracture–related phenomena, which have peak-to-valley matched fracture morphologies and have been well documented in literatures. Here, our results demonstrate another kind of widely existing crack-induced periodic corrugations and elucidate that the origin of the patterns is the regular nucleation, growth, and coalescence of nanocavities. This might provide a promising pathway toward nanofabrication by the crack-based patterning (*51*).

The multiple discrete cavitation-dominated cracking process is reminiscent of the discontinuous percolation process of shear transformation zones during the formation of a shear band in MGs (*52*), the depinning transition of cracks in disordered solids (*53*), and the stick-slip behavior of frictional instability (*54*). All these discontinuous processes in disordered systems have the nature of far from equilibrium and perhaps follow at the root of some common physical principles. The traditional continuum fracture mechanics or the sequential bond rupture mechanism (*4*, *11*, *15*) can hardly explain the organized discrete cavitation initiation ahead of the crack tip. It

Downloaded from http://advances.sciencemag.org/ on March 31, 2021

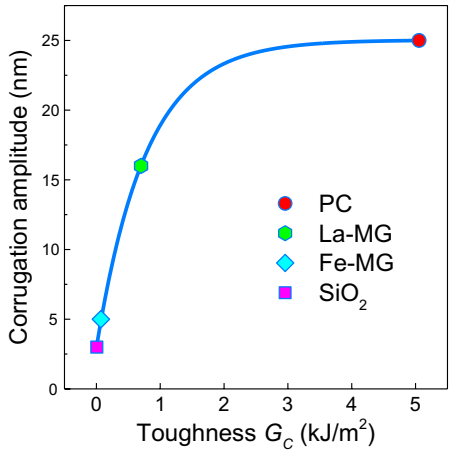

Fig. 5. Plot of the corrugation amplitude as a function of toughness. For different types of glasses with a wide range of Young's modulus E, fracture energy G_C (= K_C^2/E, where K_C is the fracture toughness) with the approximate value extracted from literatures (*1*, *23*–*25*) is used to quantify the toughness. Cavitation-induced nanocorrugations are a common feature of brittle glasses, and there is an obvious positive correlation between the amplitude of the fracture surface corrugations and the toughness. The blue curve is an exponential fit.

is also unlikely that the ordered cavitation behavior originates from the preexisting defects, e.g., grain boundaries, inclusions, and second-phase particles or pores (*4*, *15*), which are perceived as the origin of voids in the fracture of materials with nonuniform structures. Nonetheless, the occurrence of regular nanoscale cavitation nucleation suggests the existence of ubiquitous atomic-scale "defects" in the amorphous structures of glasses. As reported in literatures (*55*–*58*), there exist vacancy and interstitial-like defect structures, liquid-like sites, or soft spots in the disordered atomic structures of amorphous solids. It is believed that these defects have a great influence on the mechanical behavior of glasses (*58*). Particularly, recent simulation studies suggest that the amorphous solids have a nature of atomic-scale structural heterogeneities, which may be responsible for the intrinsic cavitation initiation ability of glasses (*36*–*44*). Namely, stress concentration ahead of the crack tip will enhance the atomic diffusion via nonaffine rearrangement and causes the spontaneous accumulation of low-density zones arising from the atomic-scale spatial fluctuation of glassy systems (*13*, *36*–*44*), thus resulting in the self-assembly cavitation initiation. The heterogeneity-related low-density zones with loose atomic packing and large free volume content can be treated as the inherent defects of glasses (*58*). In this respect, on the one hand, the amorphous nature offers glasses a uniform structure, relative to the dislocations or grain boundaries in crystals and thus endows glasses with a high strength (*24*, *26*); on the other hand, the amorphous structure of glasses is intrinsically inhomogeneous at the atomic scale (*15*, *58*), resulting in the cavitation-triggered catastrophic fracture. From this viewpoint, it is promising to tailor the heterogeneities of glasses to avoid the occurrence of cavitation-induced cracking and thus achieve glasses with sufficient ductility and damage tolerance, such as the recently reported highly ductile amorphous oxide with a dense and flaw-free atomic arrangement (*3*, *5*). From a theoretical perspective, the intrinsic heterogeneities of glasses invalidate the classical continuum understanding of dynamic crack propagation (*14*, *15*, *47*, *53*), which is based on the continuum concept of matter and is valid for the description of generic fracture on the macroscale (*4*, *11*). Therefore, further fundamental fracture theory taking into account the heterogeneities of amorphous solids needs to be undertaken to describe the nanoscale cavitation-dominated crack propagation of glasses.

In summary, we demonstrate a generalized cavitation mechanism governing the fracture of glasses. We unveil the cavitation nucleation–, growth-, and coalescence-dominated crack front propagation mode, and plastic flow exhibited by the cavitation process thus verifies the existence of ductility during the breakage of brittle glasses. Our experimental observations unravel the formation mechanism of the nanoscale fracture surface patterns of glasses and show that cavitation is the unified origin of the many elusive patterned fracture morphologies of glasses. The revealed intrinsic cavitation mechanism is important for elucidating the fundamental law of how glasses break and could provide incentives to understand the failure of other disordered systems, including mechanical instabilities of geological and biological materials.

MATERIALS AND METHODS

Sample preparation

Four typical alloys of $Fe_{78}Si_9B_{13}$, $Mg_{61}Cu_{28}Gd_{11}$, $La_{55}Ni_{20}Al_{25}$, and $Zr_{64.13}Cu_{15.75}Ni_{10.12}Al_{10}$ (in atomic %) with the normal compositions were prepared by arc-melting the constituent elements [purity: Fe, B, Mg, Gd, Ni, Zr ~99.9 weight % (wt %); Cu, Al ~99.99 wt %; Si ~99.999 wt %; La ~99.5 wt %] in a Ti-gettered high-purity argon atmosphere, respectively. Then, glassy ribbons with a thickness of ~25 μm were produced by the melt-spinning technique. The free surfaces of these ribbons were very smooth and were exempted from polishing or any other damage, facilitating the subsequent experimental characterization. The pristine PC and SiO_2 glassy plates with a thickness of ~1 mm were commercially available, and their compositions were checked by chemical analysis using inductively coupled plasma atomic emission spectroscopy. The amorphous nature of all these glass samples was verified by x-ray diffraction over scattering angles ranging from 20° to 80°, using a Bruker D8 Advance with a Cu-Kα radiation source in the Bragg-Brentano geometry. All the glass samples were ultrasonically cleaned in acetone and ethanol and blow-dried with a nitrogen gun before further experiments.

Inclined indentation cracking

Indentation cracking was produced by Vickers indentation with a diamond pyramid indenter tip in ambient atmosphere. To avoid the formation of random cracks and to achieve cracks in a controllable way on the sample surfaces, the glass samples were attached to a glass slide on an inclined substrate with an inclination angle of ~1° with respect to the horizontal plane. Under the inclined indentation with a square pyramid indenter, the higher side of the sample underwent wedge-splitting like loading and the cleavage (opening-mode) fracture consequently resulted in a V-shaped opening of the fracture surface and a crack extending from the indent corner on the higher side. For the MG and PC samples, the loading force was 500 gf, which was sufficiently high to trigger pronounced cracking. For the SiO_2 samples, the loading force was 50 gf, which was high enough to produce regular crack grooves before the emergence of shattered pieces. Cracks with different width configurations were acquired through the change of indentation strain by adjusting the indent depth.

Downloaded from http://advances.sciencemag.org/ on March 31, 2021

AFM measurements

Atomic force microscopy measurements were conducted on an Asylum Research MFP-3D AFM (Asylum Research). AFM imaging was acquired in tapping mode using the high-resolution probes (MikroMasch Hi'Res-C15/Cr-Au) with a nominal tip radius of 1 nm, a typical resonant frequency of 325 kHz, and a force constant of 40 N/m. Owing to the high spatial resolution (typical lateral resolution of ~1 nm, vertical resolution of ~0.1 nm) of the AFM measurements (*59*), 3D topographic information of the cracks after loading was captured with the AFM tip ex situ scanning perpendicular to the crack propagation direction. To gain geometry information inside the crack and topography fluctuation along the crack, scan direction of the AFM tip was adjusted to the crack propagation direction with the sample remaining stationary. Raw AFM data were processed from .ibw files using standard procedures implemented in Gwyddion (*60*).

SUPPLEMENTARY MATERIALS

Supplementary material for this article is available at http://advances.sciencemag.org/cgi/content/full/7/14/eabf7293/DC1

REFERENCES AND NOTES

1. M. F. Ashby, *Materials Selection in Mechanical Design* (Butterworth-Heinemann, 2011).
2. J. C. Mauro, Grand Challenges in Glass Science. *Front. Mater.* **1**, 20 (2014).
3. E. J. Frankberg, J. Kalikka, F. Garcia Ferre, L. Joly-Pottuz, T. Salminen, J. Hintikka, M. Hokka, S. Koneti, T. Douillard, B. Le Saint, P. Kreiml, M. J. Cordill, T. Epicier, D. Stauffer, M. Vanazzi, L. Roiban, J. Akola, F. Di Fonzo, E. Levanen, K. Masenelli-Varlot, Highly ductile amorphous oxide at room temperature and high strain rate. *Science* **366**, 864–869 (2019).
4. B. R. Lawn, *Fracture of Brittle Solids* (Cambridge Univ. Press, 2010).
5. L. Wondraczek, Overcoming glass brittleness. *Science* **366**, 804–805 (2019).
6. L. Wondraczek, J. C. Mauro, J. Eckert, U. Kühn, J. Horbach, J. Deubener, T. Rouxel, Towards ultrastrong glasses. *Adv. Mater.* **23**, 4578–4586 (2011).
7. A. Yuse, M. Sano, Transition between crack patterns in quenched glass plates. *Nature* **362**, 329–331 (1993).
8. C.-H. Chen, E. Bouchbinder, A. Karma, Instability in dynamic fracture and the failure of the classical theory of cracks. *Nat. Phys.* **13**, 1186–1190 (2017).
9. D. Massy, F. Mazen, D. Landru, N. Ben Mohamed, S. Tardif, A. Reinhardt, F. Madeira, O. Kononchuk, F. Rieutord, Crack front interaction with self-emitted acoustic waves. *Phys. Rev. Lett.* **121**, 195501 (2018).
10. M. Wang, M. Fourmeau, L. Zhao, F. Legrand, D. Nélias, Self-emitted surface corrugations in dynamic fracture of silicon single crystal. *Proc. Natl. Acad. Sci. U.S.A.* **117**, 16872–16879 (2020).
11. E. Sharon, J. Fineberg, Confirming the continuum theory of dynamic brittle fracture for fast cracks. *Nature* **397**, 333–335 (1999).
12. M. J. Buehler, Z. Xu, Materials science mind the helical crack. *Nature* **464**, 42–43 (2010).
13. A. Furukawa, H. Tanaka, Inhomogeneous flow and fracture of glassy materials. *Nat. Mater.* **8**, 601–609 (2009).
14. E. Bouchbinder, T. Goldman, J. Fineberg, The dynamics of rapid fracture: Instabilities, nonlinearities and length scales. *Rep. Prog. Phys.* **77**, 046501 (2014).
15. D. Bonamy, E. Bouchaud, Failure of heterogeneous materials: A dynamic phase transition? *Phys. Rep.* **498**, 1–44 (2011).
16. A. Nicolas, E. E. Ferrero, K. Martens, J.-L. Barrat, Deformation and flow of amorphous solids: Insights from elastoplastic models. *Rev. Mod. Phys.* **90**, 045006 (2018).
17. F. Celarie, S. Prades, D. Bonamy, L. Ferrero, E. Bouchaud, C. Guillot, C. Marliere, Glass breaks like metal, but at the nanometer scale. *Phys. Rev. Lett.* **90**, 075504 (2003).
18. B. Wang, Y. Yu, M. Wang, J. C. Mauro, M. Bauchy, Nanoductility in silicate glasses is driven by topological heterogeneity. *Phys. Rev. B* **93**, 064202 (2016).
19. J.-P. Guin, S. M. Wiederhorn, Fracture of silicate glasses: Ductile or brittle? *Phys. Rev. Lett.* **92**, 215502 (2004).
20. G. Pezzotti, A. Leto, Contribution of spatially and spectrally resolved cathodoluminescence to study crack-tip phenomena in silica glass. *Phys. Rev. Lett.* **103**, 175501 (2009).
21. A. L. Greer, Metallic glasses. *Science* **267**, 1947–1953 (1995).
22. R. O. Ritchie, The conflicts between strength and toughness. *Nat. Mater.* **10**, 817–822 (2011).
23. W. H. Wang, The elastic properties, elastic models and elastic perspectives of metallic glasses. *Prog. Mater. Sci.* **57**, 487–656 (2012).
24. B. A. Sun, W. H. Wang, The fracture of bulk metallic glasses. *Prog. Mater. Sci.* **74**, 211–307 (2015).
25. M. F. Ashby, A. L. Greer, Metallic glasses as structural materials. *Scr. Mater.* **54**, 321–326 (2006).
26. M.-X. Li, S.-F. Zhao, Z. Lu, A. Hirata, P. Wen, H.-Y. Bai, M. Chen, J. Schroers, Y. Liu, W.-H. Wang, High-temperature bulk metallic glasses developed by combinatorial methods. *Nature* **569**, 99–103 (2019).
27. D. C. Hofmann, J. Y. Suh, A. Wiest, G. Duan, M. L. Lind, M. D. Demetriou, W. L. Johnson, Designing metallic glass matrix composites with high toughness and tensile ductility. *Nature* **451**, 1085–1089 (2008).
28. A. L. Greer, Y. Q. Cheng, E. Ma, Shear bands in metallic glasses. *Mater. Sci. Eng. Rep.* **74**, 71–132 (2013).
29. S. Vernede, L. Ponson, J. P. Bouchaud, Turbulent fracture surfaces: A footprint of damage percolation? *Phys. Rev. Lett.* **114**, 215501 (2015).
30. A. S. Argon, M. Salama, The mechanism of fracture in glassy materials capable of some inelastic deformation. *Mater. Sci. Eng.* **23**, 219–230 (1976).
31. X. K. Xi, D. Q. Zhao, M. X. Pan, W. H. Wang, Y. Wu, J. J. Lewandowski, Fracture of brittle metallic glasses: Brittleness or plasticity. *Phys. Rev. Lett.* **94**, 125510 (2005).
32. Z. F. Zhang, F. F. Wu, W. Gao, J. Tan, Z. G. Wang, M. Stoica, J. Das, J. Eckert, B. L. Shen, A. Inoue, Wavy cleavage fracture of bulk metallic glass. *Appl. Phys. Lett.* **89**, 251917 (2006).
33. G. Wang, D. Q. Zhao, H. Y. Bai, M. X. Pan, A. L. Xia, B. S. Han, X. K. Xi, Y. Wu, W. H. Wang, Nanoscale periodic morphologies on the fracture surface of brittle metallic glasses. *Phys. Rev. Lett.* **98**, 235501 (2007).
34. M. Q. Jiang, Z. Ling, J. X. Meng, L. H. Dai, Energy dissipation in fracture of bulk metallic glasses via inherent competition between local softening and quasi-cleavage. *Philos. Mag.* **88**, 407–426 (2008).
35. R. L. Narayan, P. Tandaiya, R. Narasimhan, U. Ramamurty, Wallner lines, crack velocity and mechanisms of crack nucleation and growth in a brittle bulk metallic glass. *Acta Mater.* **80**, 407–420 (2014).
36. I. Singh, R. Narasimhan, U. Ramamurty, Cavitation-induced fracture causes nanocorrugations in brittle metallic glasses. *Phys. Rev. Lett.* **117**, 044302 (2016).
37. P. Murali, T. F. Guo, Y. W. Zhang, R. Narasimhan, Y. Li, H. J. Gao, Atomic scale fluctuations govern brittle fracture and cavitation behavior in metallic glasses. *Phys. Rev. Lett.* **107**, 215501 (2011).
38. C. H. Rycroft, E. Bouchbinder, Fracture toughness of metallic glasses: Annealing-induced embrittlement. *Phys. Rev. Lett.* **109**, 194301 (2012).
39. P. Guan, S. Lu, M. J. Spector, P. K. Valavala, M. L. Falk, Cavitation in amorphous solids. *Phys. Rev. Lett.* **110**, 185502 (2013).
40. T. C. Hufnagel, C. A. Schuh, M. L. Falk, Deformation of metallic glasses: Recent developments in theory, simulations, and experiments. *Acta Mater.* **109**, 375–393 (2016).
41. Q. An, K. Samwer, M. D. Demetriou, M. C. Floyd, D. O. Duggins, W. L. Johnson, W. A. Goddard, How the toughness in metallic glasses depends on topological and chemical heterogeneity. *Proc. Natl. Acad. Sci. U.S.A.* **113**, 7053–7058 (2016).
42. Y. He, P. Yi, M. L. Falk, Critical analysis of an FeP empirical potential employed to study the fracture of metallic glasses. *Phys. Rev. Lett.* **122**, 035501 (2019).
43. G. N. Toepperwein, J. J. de Pablo, Cavitation and crazing in rod-containing nanocomposites. *Macromolecules* **44**, 5498–5509 (2011).
44. Z. Ye, R. A. Riggleman, Molecular view of cavitation in model-solvated polymer networks. *Macromolecules* **53**, 7825–7834 (2020).
45. X. C. Tang, T. Nguyen, X. H. Yao, J. W. Wilkerson, A cavitation and dynamic void growth model for a general class of strain-softening amorphous materials. *J. Mech. Phys. Solids* **141**, 104023 (2020).
46. T. To, S. S. Sorensen, M. Stepniewska, A. Qiao, L. R. Jensen, M. Bauchy, Y. Yue, M. M. Smedskjaer, Fracture toughness of a metal-organic framework glass. *Nat. Commun.* **11**, 2593 (2020).
47. C. W. Barney, C. E. Dougan, K. R. McLeod, A. Kazemi-Moridani, Y. Zheng, Z. Ye, S. Tiwari, I. Sacligil, R. A. Riggleman, S. Cai, J. H. Lee, S. R. Peyton, G. N. Tew, A. J. Crosby, Cavitation in soft matter. *Proc. Natl. Acad. Sci. U.S.A.* **117**, 9157–9165 (2020).
48. B. R. Lawn, R. F. Cook, Probing material properties with sharp indenters: A retrospective. *J. Mater. Sci.* **47**, 1–22 (2011).
49. D. Jang, J. R. Greer, Transition from a strong-yet-brittle to a stronger-and-ductile state by size reduction of metallic glasses. *Nat. Mater.* **9**, 215–219 (2010).
50. J. Luo, J. Wang, E. Bitzek, J. Y. Huang, H. Zheng, L. Tong, Q. Yang, J. Li, S. X. Mao, Size-dependent brittle-to-ductile transition in silica glass nanofibers. *Nano Lett.* **16**, 105–113 (2016).
51. K. H. Nam, I. H. Park, S. H. Ko, Patterning by controlled cracking. *Nature* **485**, 221–224 (2012).
52. D. Şopu, A. Stukowski, M. Stoica, S. Scudino, Atomic-level processes of shear band nucleation in metallic glasses. *Phys. Rev. Lett.* **119**, 195503 (2017).
53. A. B. J. Chopin, A. Jog, L. Ponson, depinning dynamics of crack fronts. *Phys. Rev. Lett.* **121**, 235501 (2018).

Downloaded from http://advances.sciencemag.org/ on March 31, 2021

54. H. Kawamura, T. Hatano, N. Kato, S. Biswas, B. K. Chakrabarti, Statistical physics of fracture, friction, and earthquakes. *Rev. Mod. Phys.* **84**, 839–884 (2012).
55. L. Skuja, K. Kajihara, M. Hirano, H. Hosono, Oxygen-excess-related point defects in glassy/amorphous SiO_2 and related materials. *Nucl. Inst. Methods Phys. Res. B* **286**, 159–168 (2012).
56. J. Brechtl, H. Wang, N. Kumar, T. Yang, Y. R. Lin, H. Bei, J. Neuefeind, W. Dmowski, S. J. Zinkle, Investigation of the thermal and neutron irradiation response of BAM-11 bulk metallic glass. *J. Nucl. Mater.* **526**, 151771 (2019).
57. Y. Petrusenko, A. Bakai, I. Neklyudov, I. Mikhailovskij, S. Bakai, P. K. Liaw, L. Huang, T. Zhang, Manifestations of point and extensive defects of bulk-metallic glasses. *J. Alloys Compd.* **504**, S198–S200 (2010).
58. J. C. Qiao, Q. Wang, J. M. Pelletier, H. Kato, R. Casalini, D. Crespo, E. Pineda, Y. Yao, Y. Yang, Structural heterogeneities and mechanical behavior of amorphous alloys. *Prog. Mater. Sci.* **104**, 250–329 (2019).
59. P. Eaton, P. West, *Atomic Force Microscopy* (Oxford Univ. Press, 2010).
60. D. Nečas, P. Klapetek, Gwyddion: An open-source software for SPM data analysis. *Centr. Eur. J.Phys.* **10**, 181–188 (2012).

Acknowledgments: We thank Y. T. Sun, D. W. Ding, S. K. Su, and D. Q. Zhao for experimental assistance. **Funding:** This work was supported by the Strategic Priority Research Program of the Chinese Academy of Sciences (XDB30000000), the National Natural Science Foundation of China (52001220, 51822107, 11790291, 61999102, and 61888102), the National Key Research and Development Plan (Grant No. 2018YFA0703603), and the National Natural Science Foundation of Guangdong Province (Grant No. 2019B030302010). **Author contributions:** W.-H.W. and H.-Y.B. supervised the project. L.-Q.S. designed and performed the experiments. L.-Q.S., B.-A.S., H.-Y.B., and W.-H.W. analyzed the data. J.-H.Y., X.-C.T., and Y.-H.L. assisted in data interpretation. L.-Q.S., B.-A.S., Y.-H.L., H.-Y.B., and W.-H.W. wrote the manuscript. **Competing interests:** The authors declare that they have no competing interests. **Data and materials availability:** All data needed to evaluate the conclusions in the paper are present in the paper and/or the Supplementary Materials. Additional data related to this paper may be requested from the authors.

Submitted 17 November 2020
Accepted 10 February 2021
Published 31 March 2021
10.1126/sciadv.abf7293

Citation: L.-Q. Shen, J.-H. Yu, X.-C. Tang, B.-A. Sun, Y.-H. Liu, H.-Y. Bai, W.-H. Wang, Observation of cavitation governing fracture in glasses. *Sci. Adv.* **7**, eabf7293 (2021).

Downloaded from http://advances.sciencemag.org/ on March 31, 2021

Science Advances

Observation of cavitation governing fracture in glasses

Lai-Quan Shen, Ji-Hao Yu, Xiao-Chang Tang, Bao-An Sun, Yan-Hui Liu, Hai-Yang Bai and Wei-Hua Wang

Sci Adv **7** (14), eabf7293.
DOI: 10.1126/sciadv.abf7293

ARTICLE TOOLS http://advances.sciencemag.org/content/7/14/eabf7293

SUPPLEMENTARY MATERIALS http://advances.sciencemag.org/content/suppl/2021/03/29/7.14.eabf7293.DC1

REFERENCES This article cites 57 articles, 6 of which you can access for free
http://advances.sciencemag.org/content/7/14/eabf7293#BIBL

PERMISSIONS http://www.sciencemag.org/help/reprints-and-permissions

Use of this article is subject to the Terms of Service

Science Advances (ISSN 2375-2548) is published by the American Association for the Advancement of Science, 1200 New York Avenue NW, Washington, DC 20005. The title *Science Advances* is a registered trademark of AAAS.

Copyright © 2021 The Authors, some rights reserved; exclusive licensee American Association for the Advancement of Science. No claim to original U.S. Government Works. Distributed under a Creative Commons Attribution NonCommercial License 4.0 (CC BY-NC).

Downloaded from http://advances.sciencemag.org/ on March 31, 2021